GRAVITATIONAL EFFECTS OF ATMOSPHERIC PROCESSES IN SG GRAVITY DATA

Bruno Meurers

Institute of Meteorology and Geophysics
University of Vienna

Abstract

Some typical case studies of short term (< 120 min) gravity residual variations are investigated by comparing the air pressure signal and the residual gravity in high temporal resolution. Most of these events are connected with heavy rainfall and atmospheric processes characterized by high vertical convection activity. After almost perfect removal of even very short (< 20 min) pressure perturbations by applying a frequency independent admittance factor, a typical behavior of the gravity residuals can be observed. A common feature is a sudden gravity decrease followed by a very slow return to the previous level. Two models of vertical mass transport are used to explain the observations roughly.

Introduction

Atmospheric signatures can be detected very clearly in high quality gravity records. Gravity variations of different origin have already been interpreted e.g. by Müller and Zürn (1983) or Neumann and Zürn (1999). High temporal resolution records offer the possibility to observe gravitational effects of even very short term atmospheric processes. At the GGP station in Vienna a data set covering a period longer than 3 years is now available obtained by the superconducting gravimeter GWR C025, that is operating since August 1995. Because of the very small and linear drift of this instrument the data is especially suited for investigating such effects. Selected short term variations in gravity and air pressure channels lasting for some hours to less than 10 min have been investigated in that respect.

Data base and processing

The GWR C025 is installed on a concrete pillar in the base floor of a huge building belonging to the Central Institute for Meteorology and Geodynamics in Vienna. The institute's building is founded in tertiary sediments (loess-like clay) that form a flat topography in its immediate vicinity. The base is situated about 7-8 m below mean surface level. Thus the gravimeter sensor position is below the soil layer that can be penetrated by water after heavy rain. Unfortunately there is no ground water level sensor available in the vicinity of the station. On the other hand a lot of meteorological parameters are permanently monitored, among others precipitation data in high temporal resolution (1 min). The corresponding data acquisition system is separated by only few tens of meters from the gravity site as part of a semiautomatic climate station (TAWES). Both, the threshold - for detecting precipitation - and the precision are 0.1 mm. Precipitation events of less amount are indicated only by a specific code. The data set of GWR C025 is acquired by using the high resolution gravity channel (HR-GRAV) sampled with 1 Hz and the pressure transducer output sampled with 0.1 Hz, respectively.

Gravity residual and air pressure data have to be investigated at 1 min intervals in order to detect gravity effects of even very short term atmospheric processes. For that purpose the raw data was calibrated and decimated to 1 min samples by applying appropriate numerical FIR filters offered by the ETERNA v3.3 software (Wenzel 1996). Based on Tamura's (1987) tidal potential the gravity data set was detided using the

tidal parameters derived from the analysis of hourly data that cover a three years' interval. In order to obtain the 1 h data set several preprocessing steps were performed based on the software packages ETERNA v3.3 (Wenzel 1996) and Tsoft (Vauterin 1997). Preprocessing consisted of degapping, despiking, destepping and decimating to 1 h samples. Despiking and destepping was done automatically. Thresholds of 2 and 5 nms^{-2} respectively have been applied for spike and step detection. Manual offset corrections were necessary only in three cases of known instrumental origin. The earth tide model for the Vienna station is very well defined now. It does not differ significantly from the results obtained previously (Meurers 1998).

In a second step, air pressure effects were removed from the gravity residuals by applying an admittance factor of $-3.533 nms^{-2}/hPa$. This factor results from tidal analysis by assuming a pressure admittance factor that is constant within the tidal band. Of course, the air pressure admittance function is frequency dependent and perhaps not constant in time. Nevertheless, this method is well suited to investigate short term effects.

Case studies

A big amount of air pressure signatures have been investigated so far by comparing air pressure and residual gravity in high temporal resolution. In most cases a narrow correlation can be found even for pressure variations of less than 1-2 h duration. Generally their gravity response is almost perfectly controlled by the mean admittance factor mentioned above, although such events are often caused by very local meteorological processes which we do not expect to cause loading effects. Only sometimes a slightly higher factor is needed to remove the air pressure effect more effectively. A typical example of a cold front passage has been reported in Meurers (1999).

In addition, we found a lot of events showing very systematic residual perturbations with no or only weak correlation to air pressure variations. Three examples are shown in Figs. 1-3 comparing air pressure with gravity residuals before and after air pressure effect correction using the constant admittance factor.

The air pressure variation is quite different in these examples. In Fig. 1, air pressure is almost constant, only few perturbations of less than 1 h duration and in the order of less than 0.5 hPa can be observed. In contrast, Figs. 2 and 3 show short term pressure variations of different magnitude (up to 2 hPa) superimposed to long term trends. In all cases the air pressure effect can be perfectly removed by applying the frequency independent admittance model. In the examples shown above - and in several other cases - the gravity residuals obtained after air pressure correction show similar behavior. It is characterized by a steep residual decrease during a time interval of a few tens of minutes only. Afterwards, the residuals need some hours to return back to the previous level. A common feature of all these atmospheric events is the occurrence of heavy rainfall that was mostly connected with thunderstorms above or near the station. Another characteristic is a distinct time shift of 10 to 30 minutes between the drop of the residual curve and the begin of rainfall. The magnitude of the residual decrease (offset) is obviously well correlated with the amount of total rain fall connected with these events. This can be seen in Fig. 4. It has to be considered, of course, that only one rainfall monitoring station is perhaps not sufficient to characterize the amount of precipitation in the region, where the atmospheric process took place. This could be one reason for the scatter seen in Fig. 4.

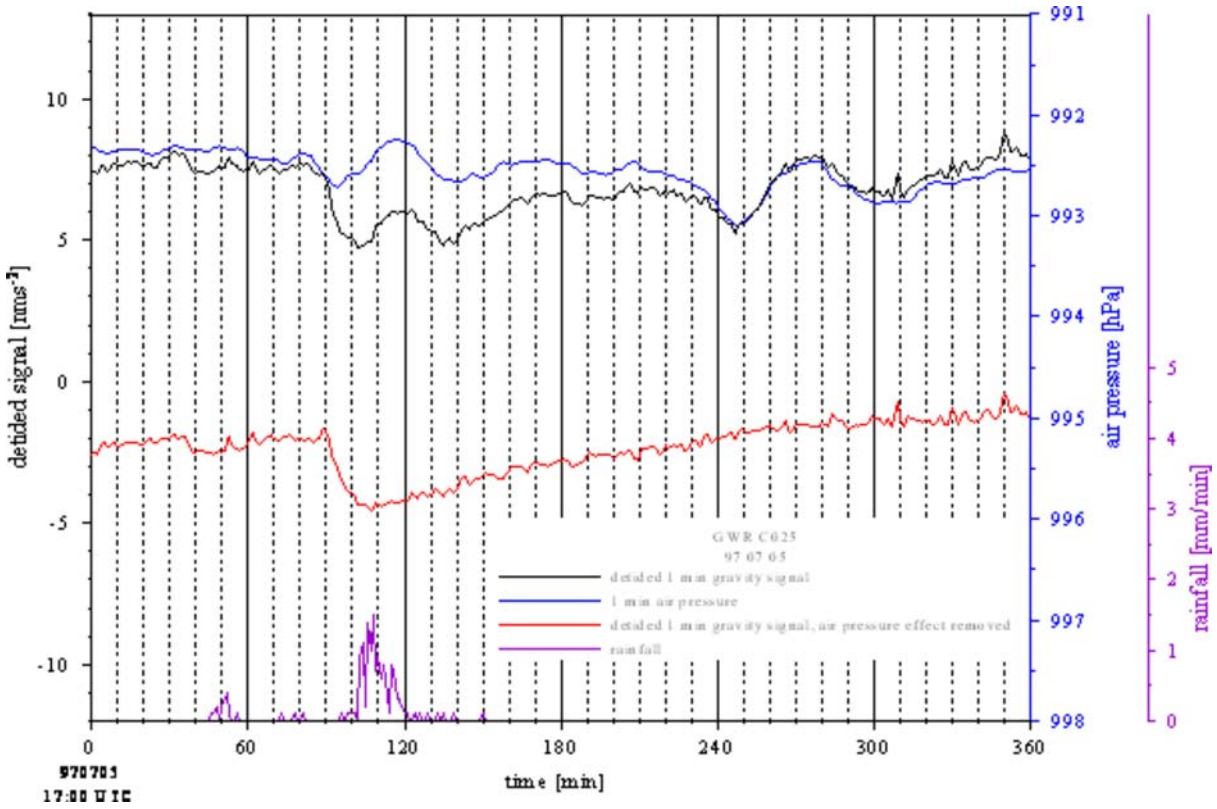

Fig. 1: Gravity residuals and air pressure observed by GWR C025 and rainfall(18-19h) in Vienna on 1997 07 05.

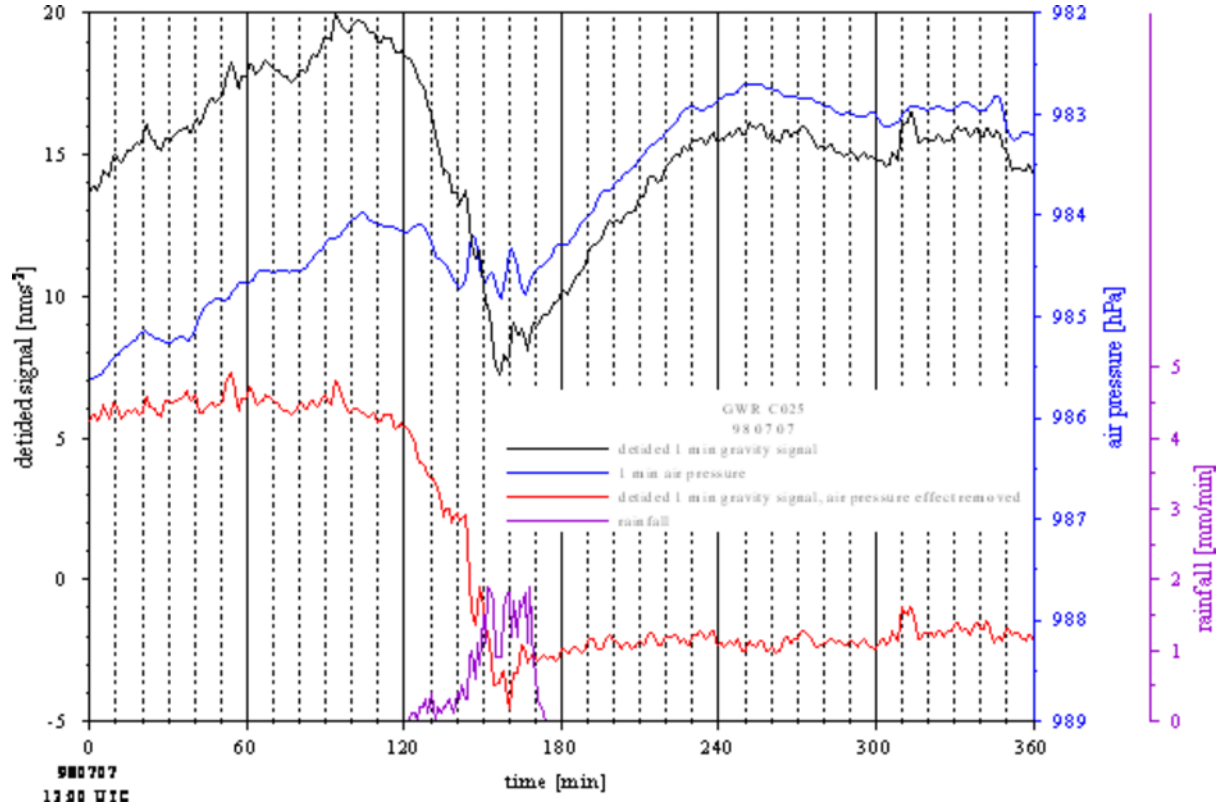

Fig. 2: Gravity residuals and air pressure observed by GWR C025 and rainfall(14:00) in Vienna on 1998 07 07.

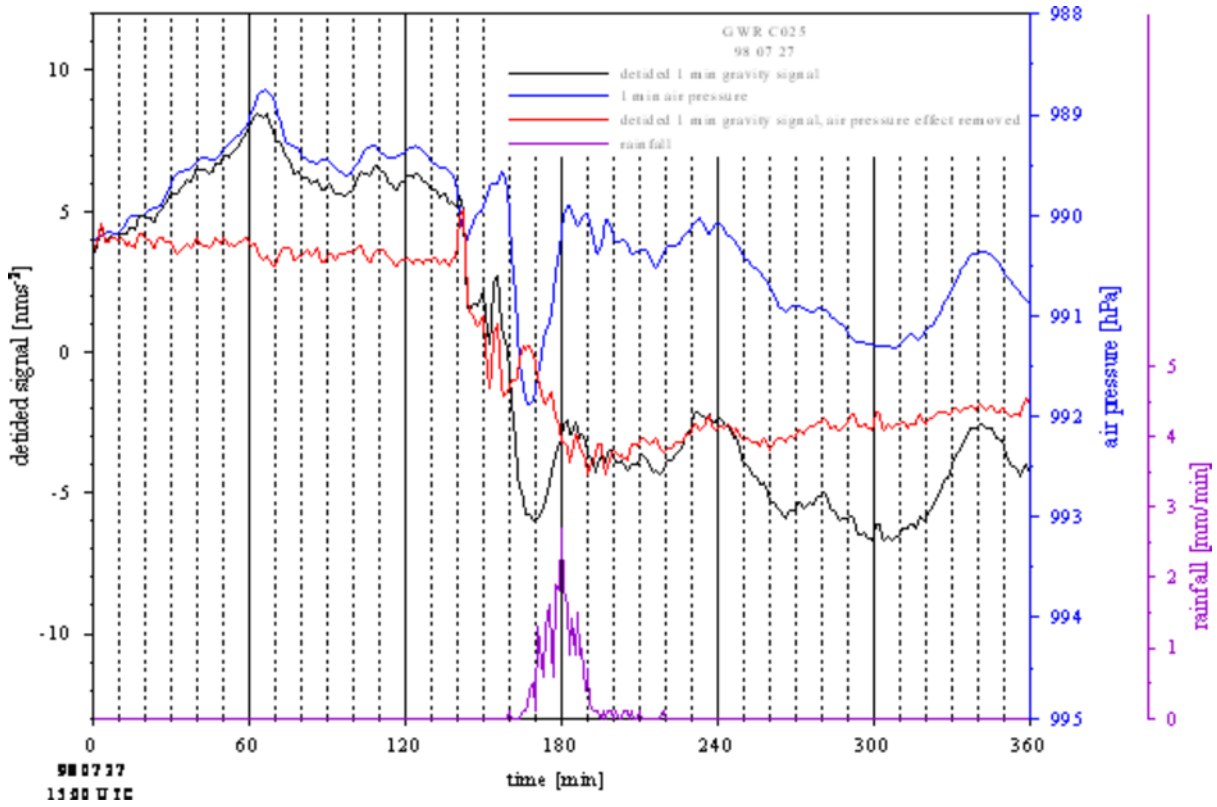

Fig. 3: Gravity residuals and air pressure observed by GWR C025 and rainfall(17:45) in Vienna on 1998 07 27.

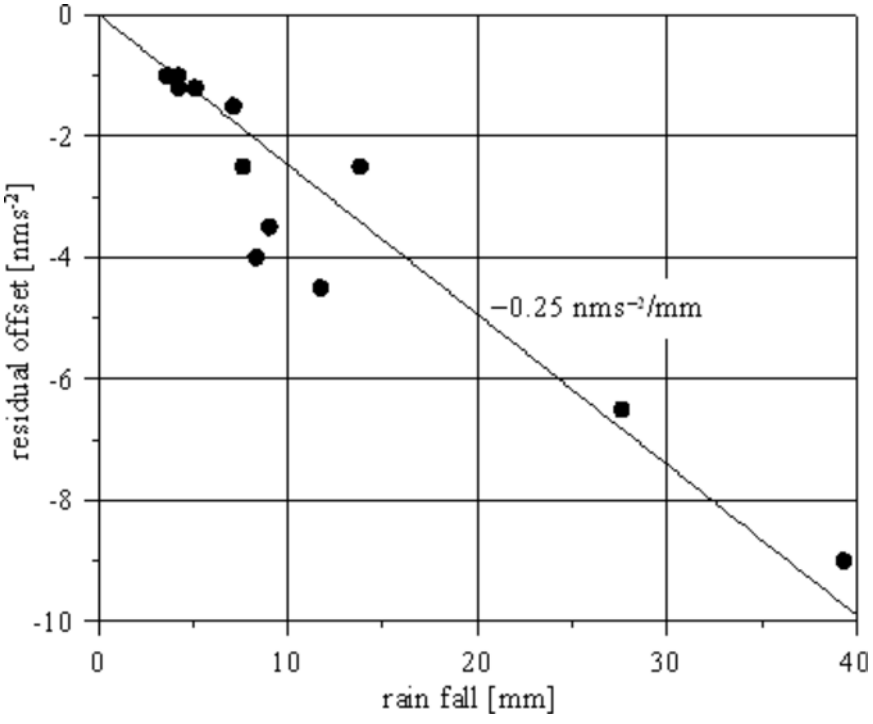

Fig. 4: Relation between gravity residual offset and total precipitation amount.

Interpretation

The gravity signals discussed above are most likely caused by vertical mass redistribution that has only small or even no air pressure effect. The fact that those events are mostly connected with thunderstorms or very heavy short term rainfall indicates atmospheric processes with a high amount of vertical convection activity. In order to give a rough estimate of the gravity effects, two very simple models have been developed that assume vertical mass flow either by air mass exchange or by water transport down to the ground.

- *Gravity effect of vertical air mass exchange without pressure variation*

The first model consists of two homogeneous cylindrical cells filled with air of different density. Both cylinders have the same radius r and vertical dimension h. At an initial state the air density is $r_0 + dr/2$ within the upper layer and $r_0 - dr/2$ within the lower layer, respectively. Therefore, the exchange of both air masses results in a density change of -dr in the upper and +dr in the lower layer.

In a coordinate system with positive z-axis pointing upwards, the gravity effect of a homogeneous vertical cylinder at the center of its lower surface is given by

$$g = 2\pi G\rho\left(h_2 - h_1 + \sqrt{h_1^2 + r^2} - \sqrt{h_2^2 + r^2}\right)$$

where h_2 is the height of the upper surface, h_1 the height of the lower surface and r the density of the cylinder. With $h = h_2 - h_1$, $h_2 = 2h$ and $h_1 = h$ for the upper cell and $h_2 = h$ and $h_1 = 0$ for the lower cell, the corresponding contributions are

$$g_u = -2\pi G\delta\rho\left(h + \sqrt{h^2 + r^2} - \sqrt{4h^2 + r^2}\right) \quad \text{and} \quad g_l = 2\pi G\delta\rho\left(h + r - \sqrt{h^2 + r^2}\right)$$

respectively. Then, the total gravity effect dg of the vertical mass transport is

$$\delta g = g_l + g_u = 2\pi G\delta\rho\left(r + \sqrt{4h^2 + r^2} - 2\sqrt{h^2 + r^2}\right)$$

The gravity effect as function of the cell radius r is shown in Fig. 5 for two models which differ in their vertical extent. In the example given here, the density contrast is 1.26×10^{-3} kgm^{-3} corresponding to an isothermal air pressure variation of 1 hPa only. For a realistic horizontal size (e.g. r between 1 and 3 km) the gravity effect is similar to the one observed in the real case studies if the density contrast is properly adjusted by a factor of 2 - 10. This yields to a density contrast that is still quite reasonable.

- *Gravity effect of vertical water mass transport*

The second model (Fig. 6f) estimates roughly the gravity effect of redistribution of water in the atmosphere. Again, it consists of two homogeneous cylindrical cells with radius r. At an initial state a certain amount of water is distributed as vapor in the upper cell between the heights h_1 and h_2. All water is transported as precipitation down to the earth surface and remains there as a cylindrical layer of radius r and height h_0. The gravity sensor is assumed to be located at the center of the water layer's lower surface.

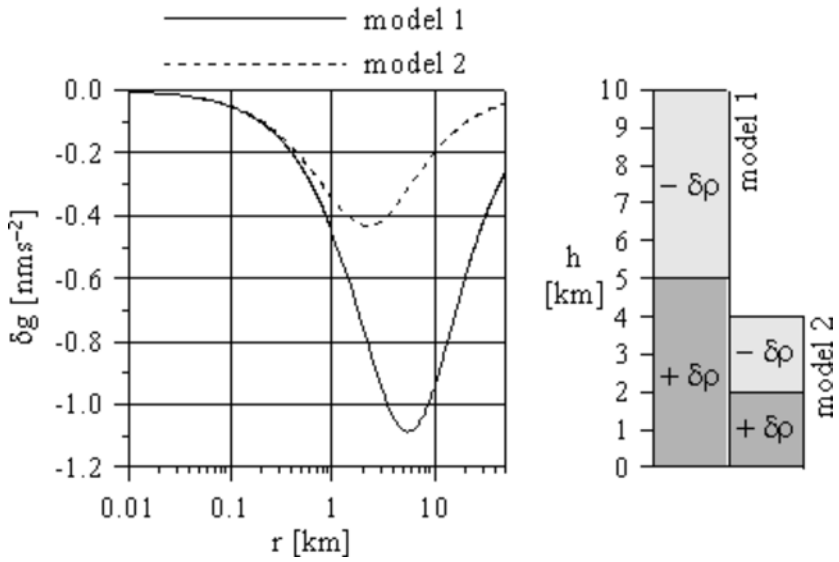

Fig. 5: Estimate of the gravity effect of a vertical air mass exchange.

As the total water mass is $m_w = \pi r^2 h_0 \rho_w$, the mean density of water and vapor within the upper cell amounts to:

$$\rho_v = \frac{m_w}{\pi r^2 (h_2 - h_1)} = \rho_w \frac{h_0}{h_2 - h_1}$$

The upper and the lower cylinder therefore contribute to the gravity at the gravimeter's sensor position (Figs. 6d and 6a) by

$$g_u = 2\pi G \rho_v \left(h_2 - h_1 + \sqrt{h_1^2 + r^2} - \sqrt{h_2^2 + r^2}\right) \quad \text{and} \quad g_l = 2\pi G \rho_w \left(h_0 + r - \sqrt{h_0^2 + r^2}\right)$$

If the gravimeter is housed in a building, the close surrounding modeled by a small disk with radius r_i around the sensor position does not contribute to gravity g_l. However, this small disk contributes most to the Bouguer plate effect. Its gravity effect g_i (Fig. 6b) has to be subtracted. If the sensor is not located immediately beneath the water layer but at a distance d downwards, then the following equation holds for the total gravity effect dg:

$$\delta g = g_l - g_i - g_u = 2\pi G \rho_w \times \left[\sqrt{d^2 + r^2} - \sqrt{(h_0 + d)^2 + r^2} - \frac{h_0}{h_2 - h_1}\left(\sqrt{(h_1 + d)^2 + r^2} - \sqrt{(h_2 + d)^2 + r^2}\right) - h_0 - \sqrt{d^2 + r_i^2} + \sqrt{(h_0 + d)^2 + r_i^2}\right]$$

Again, sign and order of magnitude of the gravity effect match observations, once a certain geometry is assumed, i.e. if the sensor is located not too close to the water layer. However, this model shows even that gravity effects of opposite sign are possible, but only for unreasonable cell sizes or if the gravity sensor is located in immediate vicinity of the lower surface of the water layer. In the latter case only the upper cylinder contributes to the gravity effect as long as a small inner disc has to be disregarded due to the station configuration. It has to be stressed, that these results are very sensitive to the assumed geometry, and reliable estimates can only be given if the layer topography with respect to the sensor location is modeled in more

detail.

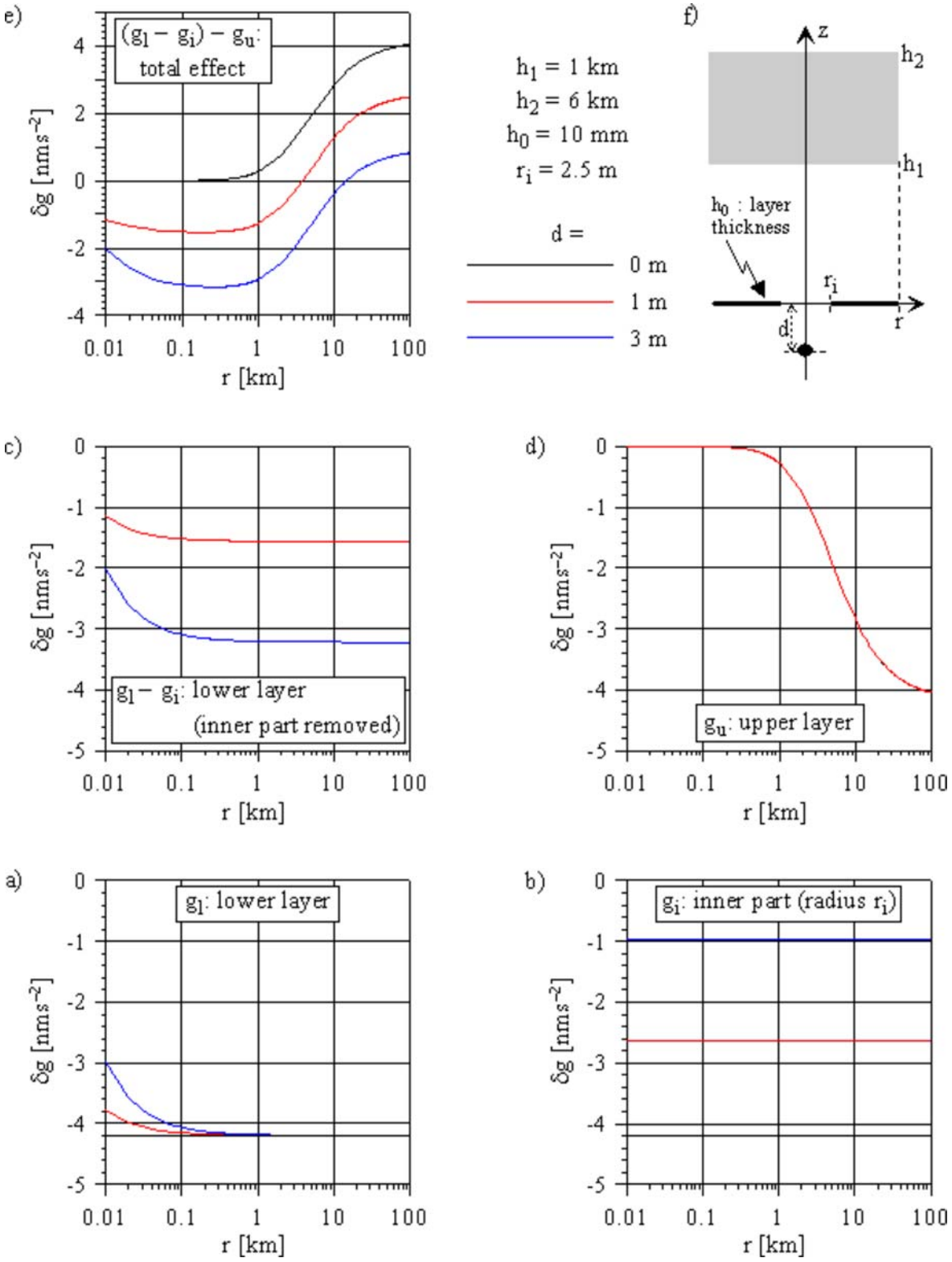

Fig. 6: Estimate of the gravity effect of vertical water mass transport. Water, equally distributed in a cylindrical cell of radius r between heights h_1 and h_2, is transported vertically down due to condensation and rain fall into a layer of thickness h_0. (a): Gravity effect of the water layer after rainfall. (b): Considering the gravimeter's surrounding, the gravity of a circular disk of radius r_i does not contribute. (c): Gravity effect of the water layer after rainfall taking (b) into account. (d): Gravity effect of the water distributed in the air before rainfall. (e): Total gravity effect at sensor position d. (f): Model geometry.

Conclusion

Both models presented above are in principle able to explain the amount of observed gravity decrease. However, the fact that the drop of gravity residual occurs 10 to 30 min before rain fall, favors vertical air convection to be the most probable interpretation. Increasing convective activity intensifies the process of water condensation and, additionally, enlarges the volume of the involved air mass. The correlation between the amount of residual offset and total rainfall can be possibly contributed to this fact. However, the presented models are rather simple. More detailed ones can be developed only if more meteorological parameters are available in the station surrounding. Nevertheless, this investigation will be continued in order to detect other influences of atmospheric processes not considered up to now.

References

Meurers, B., 1998: Gravity monitoring with a superconducting gravimeter in Vienna. In: Ducarme, B., Paquet, P. (eds): Proceedings of the 13th International Symposium on Earth Tides, Brussels 1997, 625-634.

Meurers, B., 1999: Air pressure signatures in the SG data of Vienna. In: Ducarme, B., (ed): Proceedings of the Working Group on "Analysis of Environmental Data for the Interpretation of Gravity Measurements", Jena, 1999. Bulletin d'Informations Mareés Terrestres, in press.

Müller, T. and Zürn, W., 1983: Observation of gravity changes during the passage of cold fronts. J. Geophys., 53, 155 - 162.

Neumann, U. and Zürn, W., 1999: Gravity signals from waves in the atmosphere and their modeling. Bulletin d'Informations Mareés Terrestres, in press.

Tamura, Y., 1987: A harmonic development of the tide-generating potential. Bulletin d'Informations Mareés Terrestres, 99, 6813-6855.

Vauterin, P., 1997: Graphical interactive software for the analysis of earth tide information. 13th International Symposium on Earth Tides, Brussels.

Wenzel, H.-G., 1996: The nanogal software: Earth tide data processing package ETERNA 3.30., Bulletin d'Informations Mareés Terrestres, 124, 9425-9439.

Acknowledgement

The author wishes to thank P. Melichar (head of dept.), N. Blaumoser, M. Göschke, S. Haden and R. Steiner from the Geophysical Department of the Central Institute for Meteorology and Geodynamics in Vienna for their cooperation. Rainfall data was made available by the Climatological Division of the same institute which is gratefully acknowledged.

For any request please contact: Bernard DUCARME

Observatoire Royal de Belgique

Avenue Circulaire 3
BRUSSELS B-1180
BELGIUM

Tel: +32 2 373 0248
Fax: +32 2 374 9822
